Supplementary Materials

Supplementary Table 1. Strains and plasmids used in this study.

Strains and plasmids	Description	Source
Strains		
E. coli DH5α	F⁻*ΔlacU169(Φ80 lacZ ΔM15) hsdR17 recA1 endA1 supE44*	Invitrogen
E. coli BW25113	*F-, λ-, E. coli K-12 strain BD792 (CGSC6159) lacZ*	Invitrogen
E. coli BW-△*guaB*	BW25113 strain knocked out *guaB*	This study
Plasmids		
pYB1s-ndmDCEA	StrR, araC, expression region, ndmD, T7 terminator, J23107, lac operator, ndmC, ndmE, ndmA, Trrnb, P15A-ORI	This study
pSB1c-frmAB-FDH	CmR, araC, frmA, frmB, TrrnB	This study
pYB1s-ndmDtB	StrR, araC, ndmDt1, T7 terminator, lac operator, ndmB, Trrnb, P15A-ORI	This study
pYB1s-ndmDtB(mut)	StrR, araC, ndmDt1, T7 terminator, lac operator, ndmB, Trrnb, P15A-ORI	This study

Supplementary Table 2. Primers used in this study.

Primer	Sequence
pYB1s-ndmDCEA construction	
ndmA-F	CGCGCCGTGTTAGCGCGTAATCAGAGG AGGAATTAACCGATGGAAC
ndmA-R	AGGCACGATCAAGGTCTTAGTTAGATAT AACTACGATCGCTTTCAATAACCGG
DCE-F	CTAAGACCTTGATCGTGCCTGGC
DCE-R	TTACGCGCTAACACGGCG
pSB1c-frmAB-FDH construction	
pBAD-23F	TCACACTTTGCTATGCCATAGCAT
pBAD-23R	ATCAGACCGCTTCTGCGTTCTGAT
frmA-gibson-F	GCCTGGTGCCGCGCGGCAGCCTCGAGA TGAAATCACGTGCTGCCGT
frmB-gibson-R	TCATTATATCTCCTTTCAACGCATATTCA GTTTAT
FDH-gibson-F	GTTGAAAGGAGATATAATGAAAATAGT ACTAGT
FDH-gibson-R	CCGAATTCACCACTAGTACCAGATCTTT ACTTTTTGTCGTGTTTGC
pYB1s-ndmDopB construction	
ndmB-CER	TCTTCAATAACATTGGTCAGCACGC

pYB1s-ndmDtB(mut) construction	
mutP-1-F	GTGCTGGGTCTCGGGAATTAACCATGACCAAAGCACC
mutP-1-R	GTGCTGGGTCTCGTAGCNNNNNNCCTAGGGCTGAGCTAGCCGTAAAG
mutP-2-F	GTGCTGGGTCTCGGCTAGCTGGCAGACCACAAC
mutP-2-R	GTGCTGGGTCTCGGGTCTTACTGTTCTTCTTCAATAACATTGGTCAGCAC
mutP-3-F	GTGCTGGGTCTCGGACCTTGATCGTGCCTGGC
mutP-3-R	GTGCTGGGTCTCGTTCCTCCTGTTAGCCCAAAAAACG

This study aimed to evaluate the function of the GntR family transcriptional regulator ORF4 within a *Pseudomonas* gene cluster. This gene cluster has not been extensively studied and is potentially regulated by caffeine. By fusing ORF4 with a fluorescent protein and adjusting promoter strength, the objective was to investigate ORF4's response to varying caffeine concentrations. However, the experimental strategies employed did not yield the expected results.

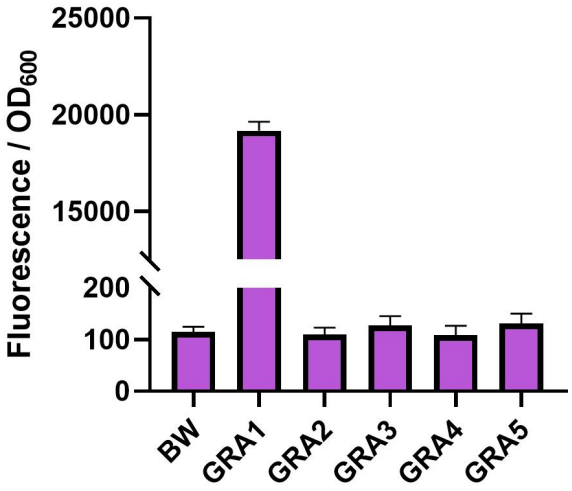

Supplementary Figure 1. Fluorescence intensity normalized by OD_{600} for different bacterial strains. The GRA1 strain showed excessive fluorescence due to weak ORF4 expression, failing to suppress the downstream ndmA promoter. In contrast, strains GRA2, GRA3, GRA4, and GRA5 exhibited reduced fluorescence due to ORF4 overexpression, which repressed the ndmA promoter. ORF4 did not demonstrate significant responsiveness to varying caffeine concentrations.

This study aimed to design a PX-specific riboswitch by modifying the previously reported theophylline-specific riboswitch sequence. The goal was to detect PX production and validate the specificity of the riboswitch under various conditions. The research revealed that incorporating rare codons into the riboswitch significantly enhanced its specificity towards theophylline, allowing the downstream expression of *codA* in the presence of theophylline. These preliminary results suggest the potential utility of the riboswitch for screening applications. Consequently, we constructed the TPR-CD2-DtB plasmid, in which the P119 promoter drives the expression of the *ndmD*, the p107 promoter drives the expression of *ndmB*, and the pBAD promoter controls the expression of the TPR-CD riboswitch. This design aimed to couple the strain's caffeine degradation capacity with its growth. However, we observed that as the concentration of 5-FC increased, the addition of TP had no significant effect on the growth of the strain. We hypothesize that the large size of the plasmid may have reduced the ability of TPR to bind theophylline and activate downstream *codA* expression, or it may have limited TPR expression. Based on these findings, we decided not to pursue the development of a PX-specific sensor using the directed evolution.

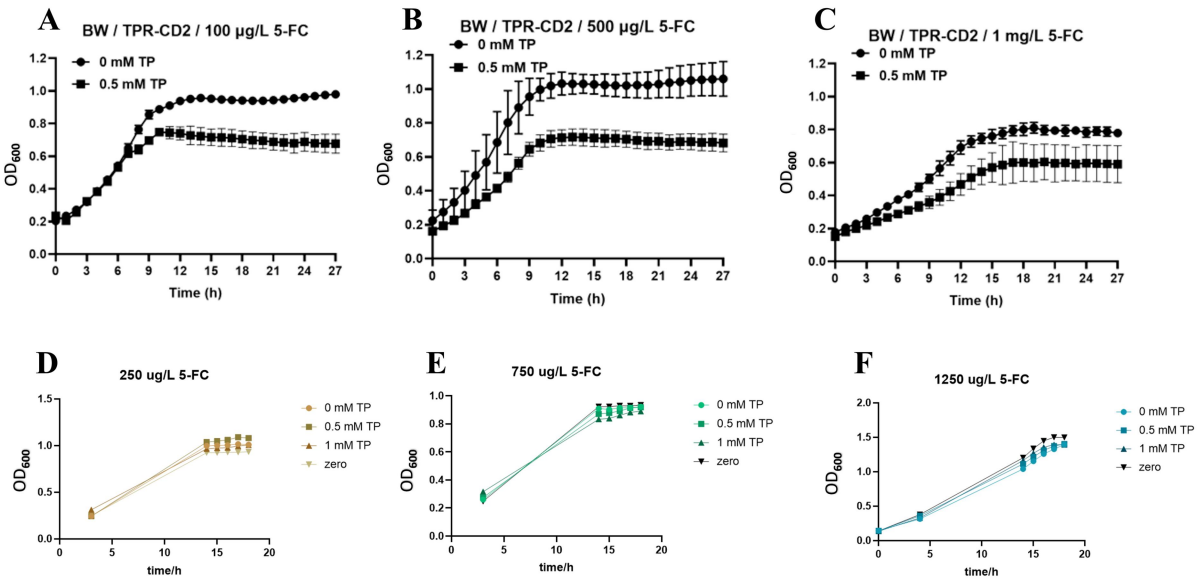

Supplementary Figure 2. (A-C) The growth of BW/TPR-CD2 strains was observed at 100, 500, and 1000 µg/L 5-FC. The results indicated that at a concentration of 500 µg/L 5-FC, the strain's growth was significantly affected by the presence of TP, suggesting the potential applicability of this system for screening purposes. **(D-F)** At 250, 750, and 1250 µg/L 5-FC, the presence or absence of TP had no significant effect on the growth of the strain.

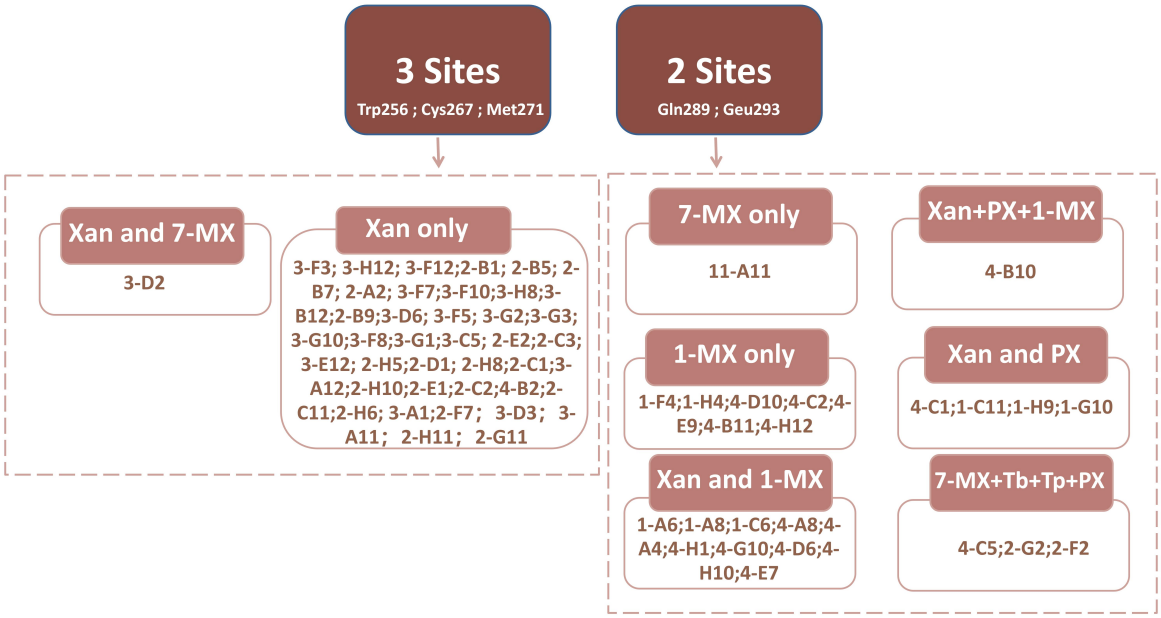

Supplementary Figure 3. This figure summarizes the mutation types and their corresponding products. Strains with higher OD_{600} values produce not only hypoxanthine but also other methylxanthine compounds (e.g., 1-MX and 7-MX). Among the mutants, those that directly produce xanthine constitute the majority.

In this study, caffeine was obtained from guarana extract, which contains approximately 22% caffeine. Due to restrictions on acquiring pure caffeine in China, an indirect method was employed to calibrate caffeine concentration using standard curves for 7-MX and theobromine[1]. The caffeine-containing guarana extract was processed through whole-cell biocatalysis using engineered *Escherichia coli*, and caffeine degradation was assessed by high-performance liquid chromatography (HPLC).

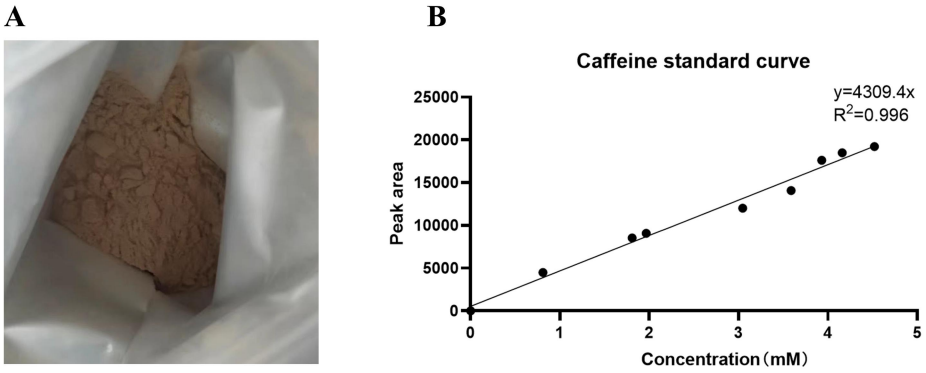

Supplementary Figure 4. (A) Guarana extract. **(B)** The standard curve of caffeine.

1. Liu, C., Wu, Y., Zhao, H., Gu, X., Gu, J., Zhao, M., Zuo, S., & Wang, P, Highly efficient Whole-Cell biocatalysis for the biosynthesis of 7-Methylxanthine and other xanthine derivatives. *ACS Sustainable Chemistry & Engineering*, 12(26), 9716–9726, (2024).

DOI: https://doi.org/10.1021/acssuschemeng.4c01165

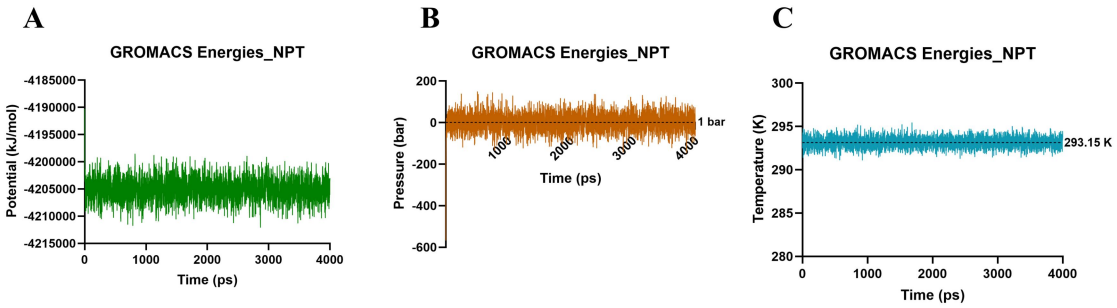

Supplementary Figure 5. Equilibrium results under NPT ensemble conditions. The simulation parameters were set to a temperature of 293.15 K, pressure of 1 bar, and pH of 7.781. **(A)** It depicts the variation in potential energy, demonstrating that the system's potential energy remains low and stable throughout the equilibration process. **(B)** It illustrates the pressure fluctuations, which, despite minor variations, remain centered around the target value of 1 bar. **(C)** It shows the temperature fluctuations, with minimal deviations and stabilization near the target value of 293.15 K.

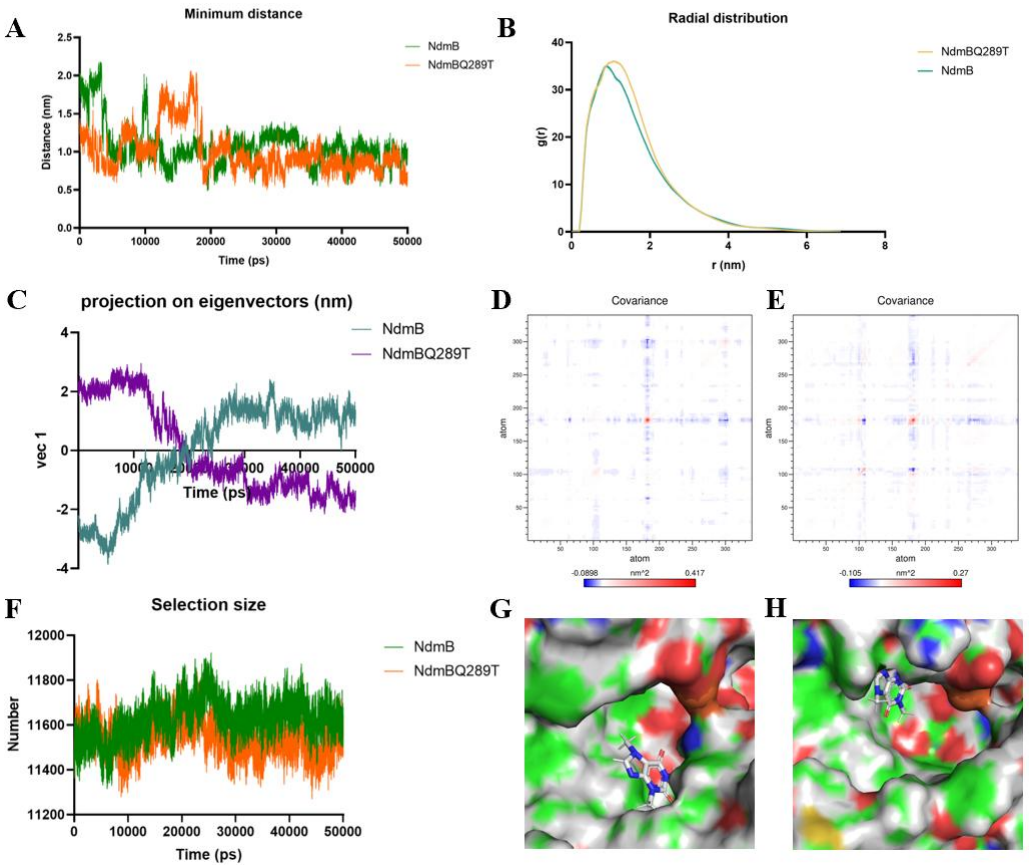

Supplementary Figure 6. Analysis between wild-type NdmB and mutant NdmB^{Q289T} with caffeine. **(A)** Distance analysis between N_3-methyl and non-heme iron: Over time, both wild-type and mutant proteins reach similar distances during the later stages of the simulation, indicating that proximity to non-heme iron is not the sole determinant of reactivity in the wild-type. **(B)** Radial distribution function (RDF) analysis: The RDF profiles of both wild-type and mutant are generally similar. However, the mutant exhibits a slightly higher peak and a more gradual decline, suggesting that the mutation results in stronger local interactions and enhanced binding stability. **(C)** Projection on eigenvectors (PCA): The PCA analysis of vec1 shows significant differences between wild-type and mutant, reflecting distinct movement patterns along the simulation timeline, indicating differing overall motion trajectories. **(D)** Covariance analysis for the wild-type: The covariance map for the

wild-type NdmB reveals relatively little positive covariance between atomic motions, suggesting weaker overall coordination of movement in NdmB. **(E)** Covariance analysis for the mutant: In contrast, the mutant shows more concentrated positive covariance, with a reduction in the negative covariance regions in $NdmB^{Q289T}$, indicating more consistent and coordinated atomic movement throughout the simulation, possibly contributing to greater structural stability. **(F)** Analysis of atoms near caffeine: The mutation affects the openness of the active site, with the mutant exhibiting a smaller interaction region compared to the wild-type. This supports the "two-pocket" hypothesis, where the mutation creates a more constrained pocket that better positions caffeine for interaction with non-heme iron, while the wild-type interacts with more residues. **(G)** Visualization of the wild-type NdmB binding pocket: caffeine is positioned in a pocket beneath the active site, with its methyl groups obstructed by surrounding residues, preventing direct access to non-heme iron. **(H)** Visualization of the $NdmB^{Q289T}$ binding pocket: caffeine is more favorably positioned in the mutant, with less steric hindrance and better alignment of the methyl group toward non-heme iron. This validates the "two-pocket" hypothesis, where the mutant creates a more direct path for interaction with non-heme iron.

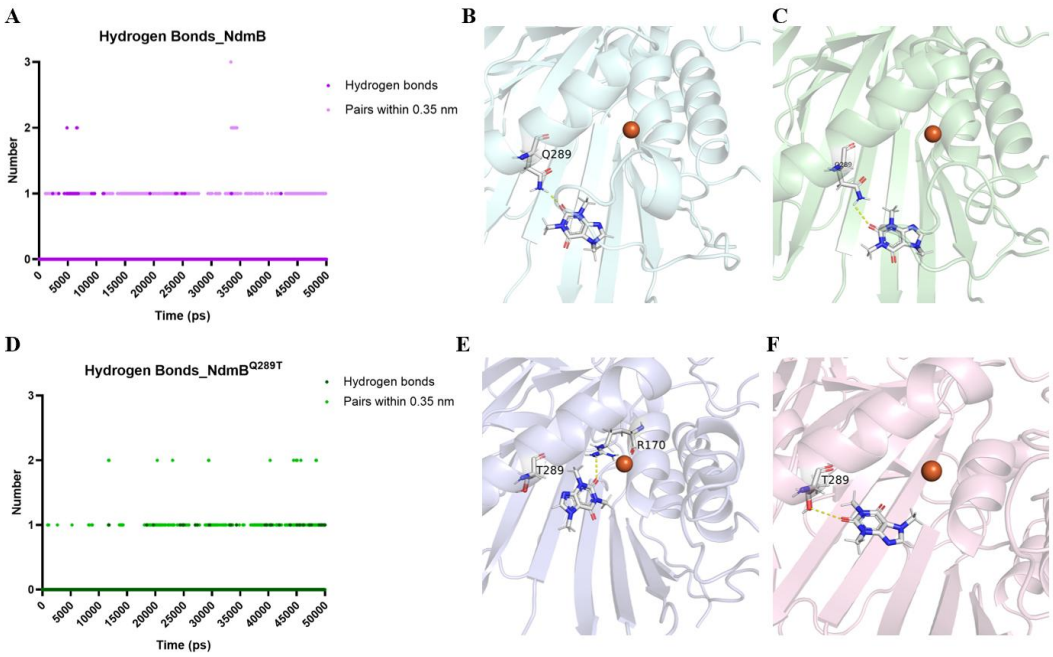

Supplementary Figure 7: Hydrogen Bond Analysis

(A) Wild-Type NdmB Hydrogen Bonds: Hydrogen bonds form primarily between 5000–7500 ps and 8500–10000 ps. **(B)** Wild-Type NdmB Structure with caffeine at 5202 ps: During the first 10000 ps, the amino hydrogen of Q289's side chain forms multiple hydrogen bonds with caffeine's carbonyl group. Repulsive forces prevent caffeine from approaching the active center. **(C)** Wild-Type NdmB Structure with caffeine at 5568 ps: Since caffeine is unable to approach the active center, it shifts towards another pocket nearby where it binds and stabilizes. However, this pocket is separated from the non-heme iron at the active center by other amino acid residues, making it difficult for caffeine to interact with the non-heme iron. **(D)** Mutant $NdmB^{Q289T}$ Hydrogen Bonds: After 40000 ps, more stable hydrogen bonds are easily formed. **(E)** Mutant $NdmB^{Q289T}$ Structure with caffeine at 45060 ps: T289 forms almost no hydrogen bonds with caffeine, and the minimal steric hindrance allows caffeine to enter the pocket and approach the non-heme iron at the active site. Once

there, the amino hydrogen of the R170 residue forms a hydrogen bond with caffeine's carbonyl group, preventing it from drifting away from the non-heme iron. **(F)** Mutant $NdmB^{Q289T}$ Structure with caffeine at 48410 ps: In addition to not obstructing caffeine's entry into the pocket, T289 generates repulsive forces when caffeine attempts to leave, helping to keep it within the pocket.